

The electrical properties of $\text{Cd}_2\text{Re}_2\text{O}_7$ under pressure

N. Barišić,¹ L. Forró,¹ D. Mandrus,² R. Jin,³ J. He,³ and P. Fazekas^{4,1}

¹*IPMC, Faculté Science de Base, EPFL, CH-1015 Lausanne, Switzerland*

²*Condensed Matter Sciences Division,*

Oak Ridge National Laboratory, Oak Ridge, TN 37831, USA

³*Department of Physics and Astronomy,*

The University of Tennessee, Knoxville, TN 37996, USA

⁴*Research Institute for Solid State Physics and Optics,*

Budapest 114, P.O.B. 49, H-1525 Hungary

Abstract

We examine the resistivity and thermopower of single crystal specimens of the pyrochlore oxide $\text{Cd}_2\text{Re}_2\text{O}_7$ at pressures up to 2GPa. Thermopower proves to be a sensitive tool in the study of the phase diagram of $\text{Cd}_2\text{Re}_2\text{O}_7$. The 200K metal-to-metal phase transition is accompanied by a strong increase of the absolute value of the thermopower. A weaker anomaly allows to identify a second phase transition at 125K. Following the temperature dependence of this anomaly, we obtain the corresponding phase boundary up to 1.2GPa, and argue that it must drop to $T = 0$ before p reaches 1.8GPa. There is a wide temperature range where the electrical properties are fairly sensitive to pressure, indicating the strong coupling of the electronic degrees of freedom to the lattice.

I. INTRODUCTION

$3d$ transition metal compounds show a variety of Mott phenomena¹, what is readily understood since for these systems, the electron–electron interaction (measured by an effective Hubbard U) is comparable to the bandwidth W . In contrast, $4d$ and, quite in particular, $5d$ transition metal compounds are supposed to be less correlated because of their relatively wide d -bands. For example, the $5d$ oxide ReO_3 is a good metal with wide d -bands.

There are, however, indications that a few $5d$ compounds also show correlation effects – or at least, they show cooperative behavior with no obvious interpretation in terms of independent electron theory. The Mott localization aspects of the low-temperature behavior of 1T-TaS_2 are long known². Recently, the interest turned towards pyrochlore oxides³. $\text{Y}_2\text{Ir}_2\text{O}_7$ is characterized as a Mott insulator¹⁰. $\text{Cd}_2\text{Os}_2\text{O}_7$ undergoes a metal–insulator transition at 220K. The phenomenon is remarkably well described as a BCS-type mean field transition which clearly involves the ordering of an electronic degree of freedom on the background of a rigid lattice^{11,12}. This led to the proposal of a Slater transition of the spins¹¹, which is further supported by evidence that charge ordering is unimportant¹². Let us note, however, that the supposed spin-density-like order parameter is experimentally not yet identified, and it would be no simple matter to postulate it because of the frustrated nature of the pyrochlore lattice¹³. Furthermore, whatever the nature of the order parameter, there is a basic difficulty: according to band theory, the Fermi surface of $\text{Cd}_2\text{Os}_2\text{O}_7$ does not seem to be nested¹⁵, and it is difficult to see how a small-amplitude order can immediately open gaps all over the Fermi surface. This difficulty alone suffices to infer that correlation effects are important.

We may generally ask what is so particular about the above cited compounds that we may consider them as correlated $5d$ electron systems. The common feature is the geometrical frustration of the transition metal sublattice (triangular lattice for 1T-TaS_2 , pyrochlore for $\text{Cd}_2\text{Os}_2\text{O}_7$). The concept of frustration was introduced for Ising antiferromagnets¹⁴, and it can be generalized to quantum magnets and Mott-localized spin-orbital systems with “antiferro” interactions. Generally speaking, frustration prevents two-sublattice order, forcing the system to choose either multi-sublattice (non-collinear) order, or spin or/and orbital liquid states. It is less obvious what frustration should mean for itinerant systems, but one can argue that it involves the suppression of kinetic energy by desctructive interference, and

the resulting enhanced importance of interaction effects. Weak coupling density wave phases tend to be eliminated and instead, local correlation effects like mass enhancement and the opening of a spin gap dominate^{24,25}.

A clear-cut example of the effect of frustration on weakly interacting electron systems is provided by the *s*-orbital Hubbard model on the pyrochlore lattice. The tight binding band structure contains a twofold degenerate zero-dispersion subband, which gives rise to marked correlation effects even in the weak coupling limit²⁶. However, flat subbands are not expected to occur in real systems. Re and Os pyrochlore oxides are more closely described by taking a *t*_{2g} tight binding model on the pyrochlore lattice; this model gives dispersive subbands. Experience with Mott-localized spin-orbital systems (modelled by the Kugel–Khomskii hamiltonian) suggests that the spin and orbital degrees of freedom play similar roles, and this should hold for correlated itinerant systems as well. Indeed, the RPA treatment of the *t*_{2g} pyrochlore Hubbard model indicates that both spin and orbital fluctuations are important, and that spin antiferromagnetism and orbital ferromagnetism are competing instabilities¹⁶.

One way to judge the importance of correlation effects is to check to which extent standard band structure calculations can account for the observed properties. The LDA electronic structure of both Cd₂Os₂O₇ and Cd₂Re₂O₇ has been determined^{15,17}. It is curious that Cd₂Os₂O₇ which has an unmistakable metal–insulator transition, appears as not particularly correlated: the specific heat coefficient γ of the metallic phase is relatively well explained by the calculated density of states $\rho(\epsilon_F)$. In contrast, there is a discrepancy between the LDA result and the measured γ for Cd₂Re₂O₇, and there is a mass enhancement factor $m^*/m = \gamma_{\text{exp.}}/\gamma_{\text{calc.}} > 1$ to account for. Actually, the two calculations give somewhat different estimates for m^*/m : Singh et al.¹⁵ imply that their $m^*/m \approx 2.4$ is not unexpected for a superconductor, i.e., that it could be due to electron–phonon coupling, while Harima¹⁷ finds $m^*/m > 5$, and concludes that Cd₂Re₂O₇ is a strongly correlated system. Optical data indicating an even higher $m^*/m \approx 20$ certainly add to the weight of evidence that electron correlation is important in Cd₂Re₂O₇¹⁸; however, the origin of the discrepancy between the specific heat and optical estimates for the mass enhancement factor remains unclear. Sakai et al.¹⁹ interpret susceptibility and NMR data as indicating localized moment character, which is synonymous with local correlations.

Taken in itself, m^*/m is probably not sufficient to allow us to decide whether either

of these pyrochlore oxides is strongly correlated; neither would such an assertion explain readily all what is seen. The large unit cell and the threefold degeneracy of the t_{2g} band are enough to show that individual subbands have to be narrow, and therefore electron–electron interaction is certainly important: it must be at least comparable to the subband widths, and also to the inter-subband pseudogaps. There is a variety of spin, and orbital, but also spin-to-orbital correlations which may become important in the range up to room temperature. Furthermore, the frustrated nature of the lattice precludes any simple ordering scenario, and therefore short-range intersite, or even multi-site, correlations have to be considered. Because of the lattice geometry, it is likely that the short-range correlated states can be envisaged as consisting of tetrahedron units with internal degrees of freedom. Such basic units of the correlated electronic state may couple to the lattice, which gives the possibility of tetramerization with the electronic degrees of freedom still fluctuating. Alternatively, the electronic degrees of freedom may become frozen into a collective state whose definition relies on the unique features of the network of tetrahedra^{20,21}. We note that the idea of “bond chirality ordering” was advocated in a recent investigation of the low temperature lattice structure of $\text{Cd}_2\text{Re}_2\text{O}_7$ ²².

Here we present the results of electrical resistivity and thermopower measurements on $\text{Cd}_2\text{Re}_2\text{O}_7$ in the pressure range 0–2 GPa. Our basic finding is that there is a wide range of temperature (roughly $60\text{K} < T < 200\text{K}$) where the electronic state of the material is “soft”, which is shown by the strong pressure dependence of the thermopower S (and to a lesser extent also of the resistivity ρ). The existence, and extreme pressure sensitivity, of the so-called second phase transition of $\text{Cd}_2\text{Re}_2\text{O}_7$ ²³, is only one aspect of this behavior. We display a phase diagram based on thermopower anomalies, including data on the pressure dependence of the second structural transition. Measuring thermopower under pressure is currently the only way to learn about the shape of that phase boundary.

II. THE PHASES OF $\text{Cd}_2\text{Re}_2\text{O}_7$

$\text{Cd}_2\text{Re}_2\text{O}_7$ is unique among the $5d$ pyrochlores inasmuch as it is the only member of this group which is known to become superconducting at $T_c = 1 - 2\text{K}$ ⁷. However, we discuss only the normal metallic phases, for which similarities and dissimilarities to other systems are of interest.

The contrasting behavior of $\text{Cd}_2\text{Re}_2\text{O}_7$ and $\text{Cd}_2\text{Os}_2\text{O}_7$ is intriguing. At room temperature T_{RT} both are bad metals with similar values of the nearly temperature independent resistivity corresponding roughly to a mean free path of the order of the lattice constant. Band structure calculation^{15,17} shows they are $5d$ semimetals with the Fermi level position corresponding to a $1/3$ -, and $1/2$ -, filled t_{2g} subband, resp. We know of no feature of the density of states, or the Fermi surface, which would obviously account for the fact that

$\text{Cd}_2\text{Os}_2\text{O}_7$ becomes an insulator at 220K, while at almost the same transition temperature $T_{\text{H}} = 200\text{K}$ $\text{Cd}_2\text{Re}_2\text{O}_7$ becomes a better metal. In the notation T_{H} , the subscript H stands for "higher", for $\text{Cd}_2\text{Re}_2\text{O}_7$ has also a "lower" transition temperature T_{L} which will be discussed later.

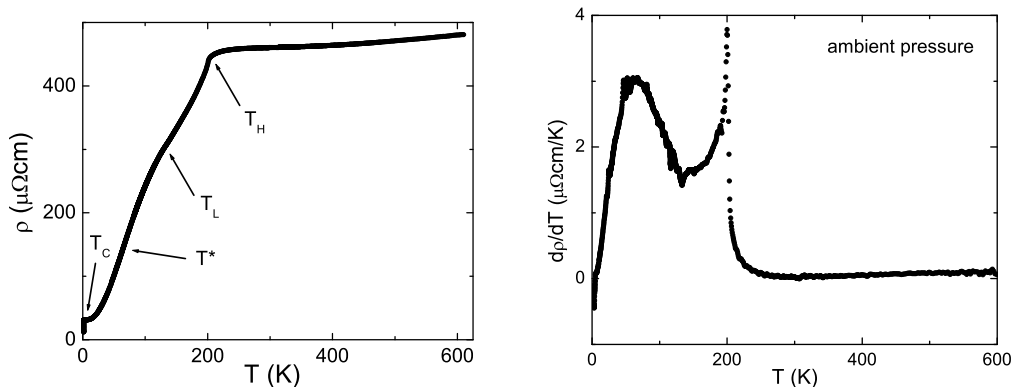


FIG. 1: *Left*: The temperature dependence of the resistivity of $\text{Cd}_2\text{Re}_2\text{O}_7$ at ambient pressure. T_{H} , T_{L} , and T_{c} signify phase transitions, while T^* marks the position of the cross-over to a low- T power law regime (see the text). *Right*: The derivative of the resistivity.

We illustrate the character of the phase transitions of $\text{Cd}_2\text{Os}_2\text{O}_7$ by the results of our measurements of the temperature dependence of the resistivity at ambient pressure (Fig. 1, left). We note that none of the previous measurements were carried up to 600K. The extended temperature scale makes the fundamental change in the character of $\text{Cd}_2\text{Os}_2\text{O}_7$ at $T_{\text{H}} = 200\text{K}$ clear. The high- T phase is a bad metal, with a resistivity which at first seems to saturate at $\sim 500\mu\Omega\text{cm}$, but then picks up again.

Decreasing the temperature through $T_{\text{H}} = 200\text{K}$, the system becomes a good metal. The low- T normal state resistivity³² extrapolates to $30\mu\Omega\text{cm}$. The resistivity change around $T_{\text{H}} = 200\text{K}$ could be compatible either with a change in the scattering mechanism, or a

change in carrier concentration, or a combination of both. Whether a phase transition occurs, has to be decided from other measurements.

Closer examination of the resistivity (ρ) versus T plot reveals that the slope passes through a maximum, a minimum, and reaches a maximum again at T_H , thus plotting $d\rho/dT$ vs T readily offers the possibility of identifying characteristic temperatures as either extrema, or zeroes, of the derivative. We illustrate this with our data shown in Fig. 1 (right). The high-temperature peak belongs to the bad-metal-to-good-metal transition at T_H . It was mentioned in³⁸ that the low-temperature hump at $T^* \approx 60\text{K}$ is also significant; however, it does not belong to a phase transition. Rather, it is a crossover temperature where the low- T $\rho(T)$ begins to follow a power-law behavior whose form will be discussed later. It is clear that other features (e.g., the minimum of $d\rho/dT$) might have been selected. However, the status of such "characteristic temperatures" is somewhat uncertain, and we need further evidence to suggest that the properties of the system undergo substantial changes at any of these points.

The continuous bad-metal-to-good-metal transition of $\text{Cd}_2\text{Re}_2\text{O}_7$ at $T_H = 200\text{K}$ is clearly seen in resistivity, susceptibility, and specific heat measurements. There is no magnetic ordering²⁷. X-Ray scattering finds new Bragg peaks, with an accompanying anomaly in the intensity of fundamental reflections. Though at first it was tentatively described as a cubic-to-cubic phase transition, there is now evidence that the symmetry is lowered to tetragonal. However, the deviation from the cubic structure is quite small, only about 0.05%^{22,37}.

Evidence that a second phase transition occurs at ambient pressure at $T_L \approx 120\text{K}$ ("L" stands for "lower"), was presented by Hiroi et al²³. They present a magnified image of the ρ versus T plot which reveals a minute hysteresis loop of a few K width in this region. The transition has little effect on the resistivity, no known signature in the susceptibility, and the specific heat shows merely an anomaly which is two orders of magnitude weaker than the one associated with the 200K transition. Clearer evidence comes from magnetoresistivity measurements which show that, after $\Delta\rho$ essentially vanishes by the time T reaches 100K, it reappears and becomes quite anisotropic from 120K onwards. Looking at the magnetoresistivity, it is plausible that the metallic state between 100K and 200K is different from that below 100K. Thus $\text{Cd}_2\text{Re}_2\text{O}_7$ should have two good metallic phases in addition to the bad metal above $T_H = 200\text{K}$. The first thermopower data³⁰ are compatible with this scenario.

Whatever the nature of the second phase transition, it is very weak. X-Ray diffraction

shows an anomaly in the temperature dependence of the fundamental reflections, including a jump for 008²³. A recent refinement²² yielded the suggestive picture of distorted tetrahedra with three unequal Re–Re distances on each triangular plaquette. The order of the bonds allows to define a bond chirality parameter for each triangle, and it turns out that the low- T structure of Cd₂Re₂O₇ can be thought of as “ferrochiral”. Thus the 120K transition involves a change of symmetry, but it is, strictly speaking, not symmetry breaking: it does not belong to a symmetry lowering (i.e., choosing a subgroup of the original symmetry group) from the $T > 120$ K phase, but to replacing one symmetry element with another. This symmetry characterization is compatible with the idea that the transition at T_L is of first order.

It is not clear what really happens at either the T_H or the T_L phase transition; in particular, whether there is an electronic order parameter coupled to the obvious structural ones. Though the symmetry changes are marked, we should not forget that they are realized by quite minute³³. distortions of the high- T cubic structure; thus though both phase transitions are literally structural transitions, it is not obvious that the structural change is enough to explain the drastic changes in electrical properties. In other words, we still have to search for the concomitant change of the many-electron state, which might well be the primary phenomenon. The X-Ray study indicates that the temperature dependence of the new Bragg peaks is anomalously slow³⁷, which would be compatible with the idea that the structural order parameter is secondary, induced by some underlying electronic order parameter. Re NQR and Cd NMR reveal that the local environment of the Re site loses trigonal symmetry at T_H , and that the character of orbital fluctuations changes at T_L ^{27,28}. XPS indicates that the t_{2g} bands are split at low T ²⁹. All the evidence points to significant rearrangement of the t_{2g} subbands, with consequent changes in their occupation, starting from T_H , and continuing until well below T_L . We envisage an itinerant version of orbital ordering transitions citefootnote5.

Certainly there is ample motivation to seek a more complete characterization of the three normal metallic phases.

Extending the measurements to higher pressures often proves enlightening. Hiroi et al measured the resistivity under the pressure of 1.5GPa, and at five high-pressure values between 3 and 8GPa⁸. 3.5GPa suffices to suppress the major structural phase transition at T_H . The weak transition at T_L seems more sensitive to pressure. A single data point published in the less known⁹ indicates that T_L is suppressed to zero somewhere beyond

2GPa. Mapping out the boundary between the two good metallic phases is an outstanding issue.

Here we present new data about the resistivity ρ and thermopower S of good-quality single crystal specimens of $\text{Cd}_2\text{Re}_2\text{O}_7$ under pressure. For resistivity, we have more pressure values up to 2GPa than in previous works, and at ambient pressure, we have extended the measurement to 600K. Our thermopower data reveal the highly anomalous nature of the "good metallic" phases of $\text{Cd}_2\text{Re}_2\text{O}_7$. At ambient pressure, our thermopower vs T curve has a much better resolved anomaly at the lower phase transition than the recently published³⁰, allowing to identify it as a secondary minimum. We performed the first measurements of thermopower under pressure, and present a pressure–temperature phase diagram based on them, including new results on $T_L(p)$. We find a distinctive feature of the intermediate temperature range $T^* < T < T_H$: it is where electrical properties are remarkably sensitive to pressure. It stands to reason that this is a regime of continuing rearrangement of $5d$ subbands where the electron–lattice interaction is particularly important. In contrast, the low-temperature ($T < T^*$) good metal, and the high-temperature ($T > T_H$) bad metal, are essentially pressure-insensitive.

III. RESULTS AND DISCUSSION

Single crystal specimens of $\text{Cd}_2\text{Re}_2\text{O}_7$ were grown using a vapor-transport method which is described in detail elsewhere³¹. The crystal was cut in smaller pieces of rectangular parallelepiped shape with the dimensions 1.5x0.25x0.025mm. After placing four contacts on the sample, it was mounted on a homemade thermopower sample holder, which fits into a clamped pressure cell. Small metallic heaters installed at both ends of the sample generated the temperature gradient measured with a Chromel-Constantan differential thermocouple. The pressure medium used in this study was kerosene, and the maximum pressure was 2GPa. The pressure was measured using a calibrated InSb pressure gauge.

The temperature dependence of the ambient-pressure resistivity of a single-crystal specimen of $\text{Cd}_2\text{Re}_2\text{O}_7$ was shown in Fig. 1(left). We stress that previous measurements did not extend up to 600K. Right above the $T > T_H$ transition, the resistivity appears to have saturated, but the extended scale shows up a further increase with temperature. It strikes the eye that the high- T resistivity is not linear in T ; this is also brought out by the enlargement

of the high- T part of the derivative plot (Fig. 2, left). For $T \geq 400\text{K}$, the resistivity seems to follow a T^2 -law (Fig. 2, right). The shape of the ρ vs T curve deviates from what one would expect from the phonon mechanism, and we ascribe it to inter-orbital (or inter-subband) scattering.

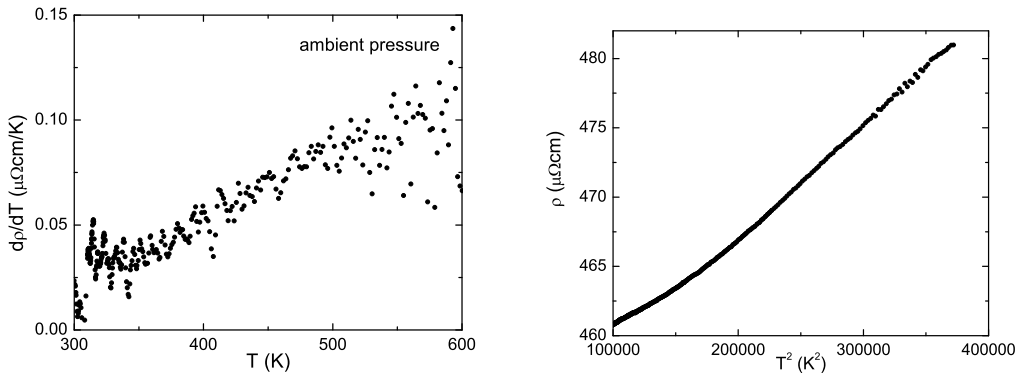


FIG. 2: The high temperature resistivity. *Left*: $d\rho/dT$ shows that ρ is not linear in T . *Right*: a ρ versus T^2 fit is successful in the range 400K–600K.

We refer also to the $d\rho/dT$ derivative plot shown in Fig. 1 (right). The continuous metal-to-metal transition at $T_H = 200\text{K}$ is marked by a strong peak of the derivative which is known to correlate with the susceptibility and specific heat anomalies³⁸. The overall $T < T_H$ behavior is similar to that known from previous measurements. The derivative plot $d\rho/dT$ vs T shows three characteristic temperatures. The large peak on the high- T side could serve to define T_H , but we prefer the definition from the derivative of the thermopower. The broad, nearly pressure-independent hump at $T^* \approx 60\text{K}$ marks the boundary between two regimes within the same low-temperature phase. There is also a recognizable minimum between these two maxima; at $p=1\text{atm}$, it is a rather sharp feature at $\sim 130\text{K}$, and happens to lie near the second transition temperature T_L which we identify from thermopower data. However, we discard the possibility of identifying T_L from this anomaly. The reason is that a minimum in $d\rho/dT$ continues to show up at all pressures, while there are good reasons to think that the second phase transition is completely suppressed before p reaches 1.8GPa.

The normal-state residual resistivity is $30\mu\Omega\text{cm}$, similar to the value given in⁸, but about a factor of 2 higher than the value quoted in²³, and in³⁰. The cooling/heating rate in our measurements was $\approx 0.6\text{K/min}$, six times faster than in the measurements of Hiroi et al²³.

This might be the reason why we did not see hysteresis in either resistivity or thermopower, though we have a fairly dense set of data points with little scatter in the relevant range of T . Nevertheless, we agree with the suggestion that the second phase transition is weakly first order.

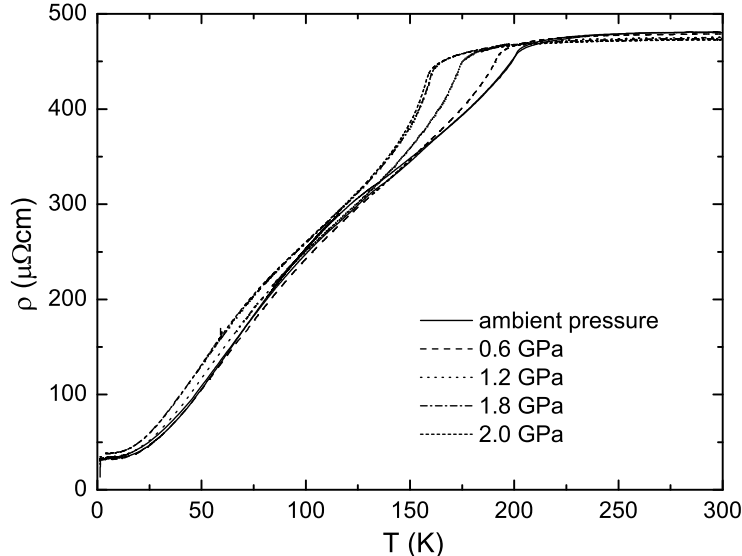


FIG. 3: The temperature dependence of the resistivity of $\text{Cd}_2\text{Re}_2\text{O}_7$ for several pressures. The sharp downturn occurs at T_{H} .

We carried out measurements at pressures of $p = 1\text{atm}$, 0.6, 1.2, 1.8, and 2GPa. The temperature dependence of the resistivity ρ for different pressures (up to 300K) is shown in Fig. 3, the derivative curves in Fig. 4, while the thermopower S is shown in Fig. 5.

The thermopower is negative at all temperatures/pressures. The T_{H} phase transition has, at any pressure, an even more spectacular signature in the thermopower than in other quantities measured before. It is associated with a steep decrease of S , which continues until at $T^* \approx 60\text{K}$ S reaches a minimum at which $|S|$ is about a factor of 10 higher than at $T = T_{\text{H}}$. Below T^* , S tends to zero in an approximately pressure-independent manner. Our thermopower data allow identifying three distinct regimes of temperature: (i) both ρ and S are essentially pressure-independent up to T^* ; (ii): the thermopower is quite sensitive to pressure at $T^* < T < T_{\text{H}}$; (iii): S and ρ are again essentially pressure-independent in the high-temperature ($T > T_{\text{H}}$) regime. Regime (ii) is the same where X-ray studies indicate

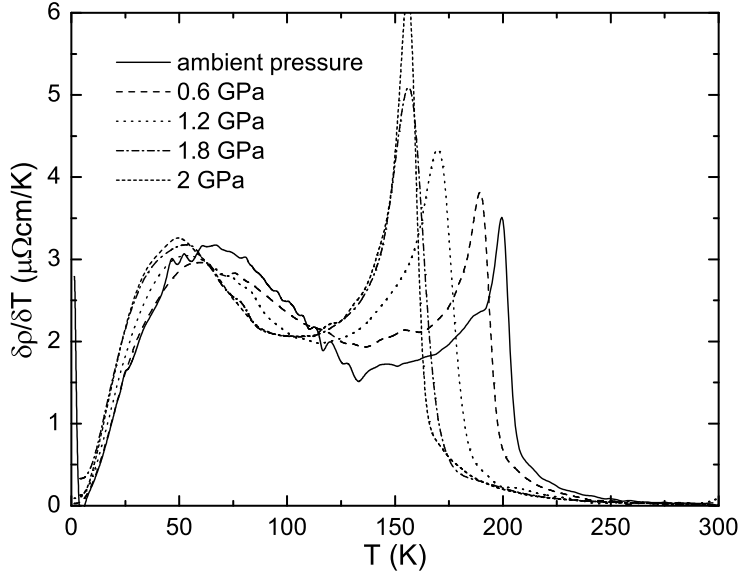


FIG. 4: The temperature dependence of the derivative of the resistivity $\partial\rho/\partial T$ for several pressures.

an anomalously slow T -dependence of the structural order parameter. The second phase transition, whenever found, sits in the middle of (ii).

Let us note that the overall value of the thermopower is rather small: $|S|$ never exceeds $10\mu\text{V}/\text{K}$. Some $5d$ elements have higher thermopower than this, and one might have expected that the narrower d -bands of our oxide give rise to a larger thermopower. However, T -dependent partial cancellation between hole-like and electron-like contributions may explain the observations. The degree of cancellation is smaller in the $T < T_{\text{H}}$ phases; this may be compatible with the disappearance of the heavy hole pocket found in the high-temperature (cubic phase) band structure¹⁵. It may also explain why we do not find the straightforward metallic behavior $S \propto T$ at $T > T_{\text{H}}$; in fact, it is rather better described by $S \propto T^2$ (see Fig 6).

Some features are more clearly seen in the derivative plot dS/dT (Fig. 7). The T_{H} transition is well defined by the cusp of dS/dT . This may seem arbitrary, but we may bring the following argument: Loosely thinking of the thermopower as a measure of the electronic entropy, finding an anomaly in dS/dT is like finding an anomaly in the specific heat. In any case, the peak positions of dS/dT and $d\rho/dT$ are lying pretty close (Fig. 8). It is remarkable that the dS/dT peak gets *sharper* under pressure. (A similar observation was made about

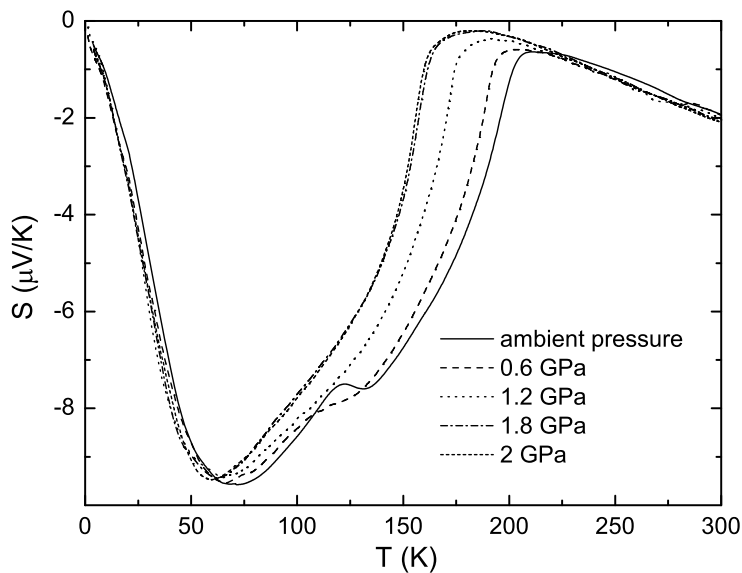


FIG. 5: The temperature dependence of the thermopower S for several pressures.

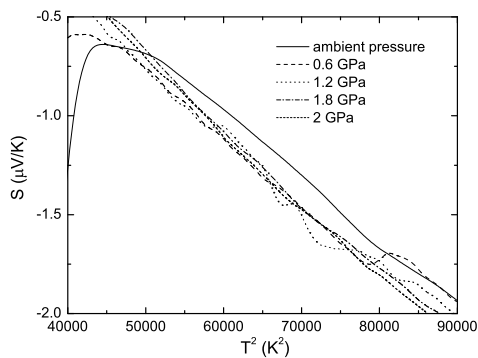


FIG. 6: Thermopower vs T^2 in the temperature range above T_H .

the ρ vs T curves in⁸.)

The second phase transition shows up in the S vs T plot (Fig. 5). At ambient pressure, there is a sizeable dip in S at about 120K, followed by a secondary minimum at ≈ 130 K. Let us observe that if we imagine the S -anomaly sharpened (the bump and the dip getting closer, without reducing their amplitudes), it would be consistent with a discontinuity of $\Delta S \approx -1\mu\text{V/K}$ (Fig. 9, left). It suggests that we center the phase transition at the point of inflection between the bump and the dip, in other words at the local minimum of

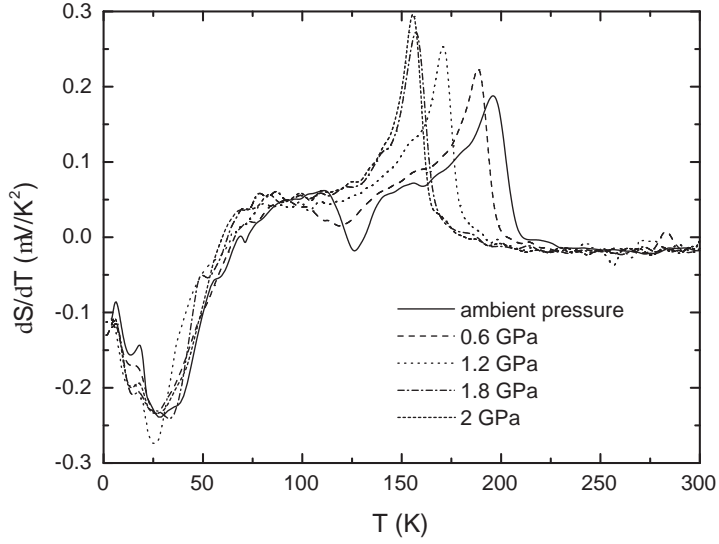


FIG. 7: The temperature dependence of the derivative of the thermopower $\partial S/\partial T$ for several pressures.

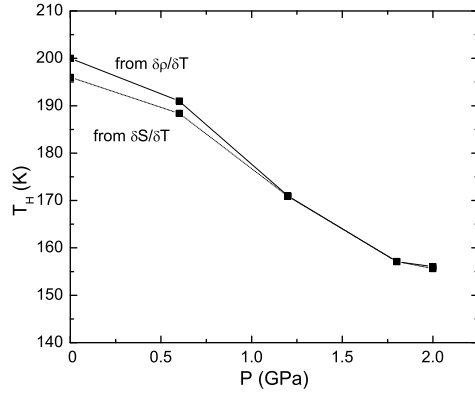


FIG. 8: Using the peak positions of either dS/dT or $d\rho/dT$ gives close-lying estimates for T_H .

dS/dT . This would be consistent with regarding the thermopower anomaly as the sign of a smeared-out (and very weak) first order transition, confirming Hiroi *et al*²³. We note that a thermopower discontinuity is associated with some first order electronic transitions, such as the valence transition of YbInCu_4 ³⁹.

The phase transitions shift under pressure: T_H drops to 156K under 2GPa (this is a less step decrease than that seen in⁸ where $T_H(2\text{GPa}) \approx 130\text{K}$. This reflects a difference in

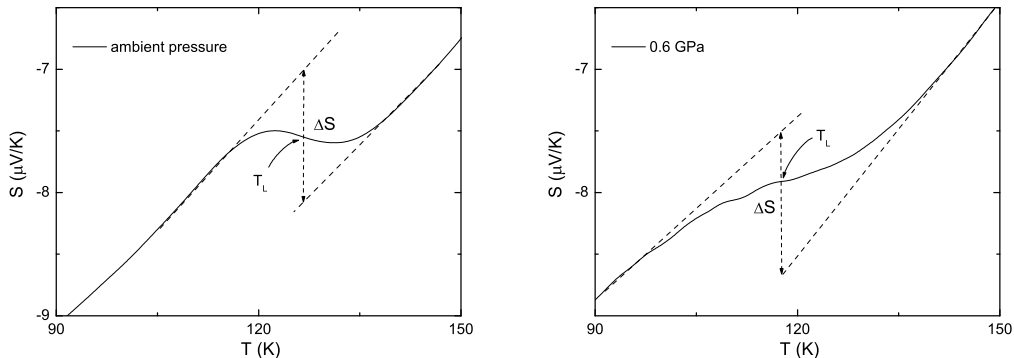


FIG. 9: Tentative interpretation of the S-shaped thermopower anomaly as a smoothed-out discontinuity for 1 bar (left), and for 0.6GPa (right).

sample quality, a point to which we return later). We already commented on the apparently increasing sharpness of the transition. The T_L transition gets suppressed rather fast under pressure. At 0.6GPa the dip-and-bump complex seems just to have shrunk to a point of inflection (Fig. 9, right): the local minimum of dS/dT reaches 0 at 115K (Fig. 7). At 1.2GPa there is not even a point of inflection, but one may still risk identifying the bottom of a valley in dS/dT at ≈ 105 K. The thermopower curves are perfectly smooth in the region $T^* < T < T_H$ at higher pressures, thus the second phase transition certainly vanishes somewhere below 1.8GPa.

Now we return to our resistivity data. The $T > T_H$ resistivity is large, essentially pressure-independent, and increases slowly with T , indicating the presence of a strong scattering mechanism specific to the pyrochlore structure. The high-temperature phase is cubic, thus the restoration of the orbital degree of freedom gives an extra scattering mechanism³⁶.

The observed lack of a magnetic field dependence of the thermopower also indicates that spin disorder scattering is not important in $\text{Cd}_2\text{Re}_2\text{O}_7$ ³⁰.

Below T_H the resistivity begins to decrease sharply, following a roughly linear T -dependence down to about 50K, below which it bends over into a seemingly power-law regime which has been fitted either with T^2 or with T^3 dependences^{7,8,30}. $\rho = \rho_0 + A_2^* T^2$ with an enhanced value $A_2^*/A_2 \propto (m^*/m)^2$ would be considered typical of strongly correlated systems, and it would be expected to show up here, since the specific heat shows enhancement. However, we found that the T^2 law would give an acceptable fit only in a narrow range of T , and even then at low pressures only (Fig. 10). In agreement with previous work⁷,

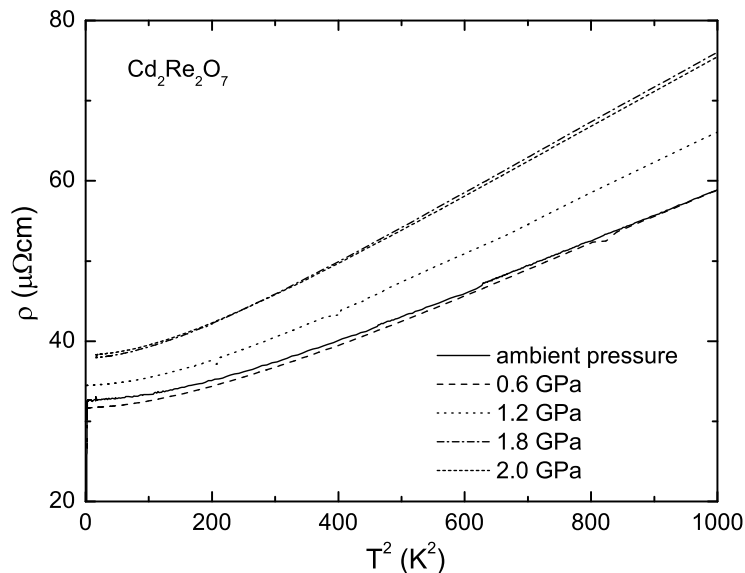


FIG. 10: The resistivity in the range 1–30K, plotted as a function of T^2 .

we find that a $\rho = \rho_0 + A_3 T^3$ fit works better (Fig. 11). The T^3 -law is to be ascribed to electron–phonon rather than to electron–electron scattering. We did not attempt to fit with a combination of T^2 - and T^3 -like terms. Undoubtedly one would find a T^2 contribution, but certainly not so large as to satisfy the Kadowaki–Woods relation.

The pressure dependence of ρ_0 and A_3 is given in Fig. 12. A moderate increase in A is compatible with increased electron–phonon interaction in a compressed lattice. We call attention to the fact that the pressure dependence of ρ_0 is quite weak, even at 2GPa we find less than $40\mu\Omega\text{cm}$. This is to be contrasted with the results of Hiroi et al. who find an about sixfold increase in ρ_0 at 1.5GPa, and a twofold increase in A_2^* . The authors of Ref.⁸ would agree that correlation, as manifested in A_2^* , is weak at ambient pressure, but argue that its role is increasing at higher pressures. Our pressure range is limited to 2GPa, but within this range, we do not detect a tendency towards heavy fermion behavior. Obviously, there is sample dependence in the observed behavior; we think that the weak pressure dependence of ρ_0 is an indication of the good quality of our samples.

There is apparent difficulty in deciding what happens to the electronic structure below 200K. The difficulty may arise partly from trying to reduce everything to a single number, the enhancement factor of the effective density of states $z^{-1} = \mathcal{N}^*(\epsilon_F)/\mathcal{N}(\epsilon_F)$, which would

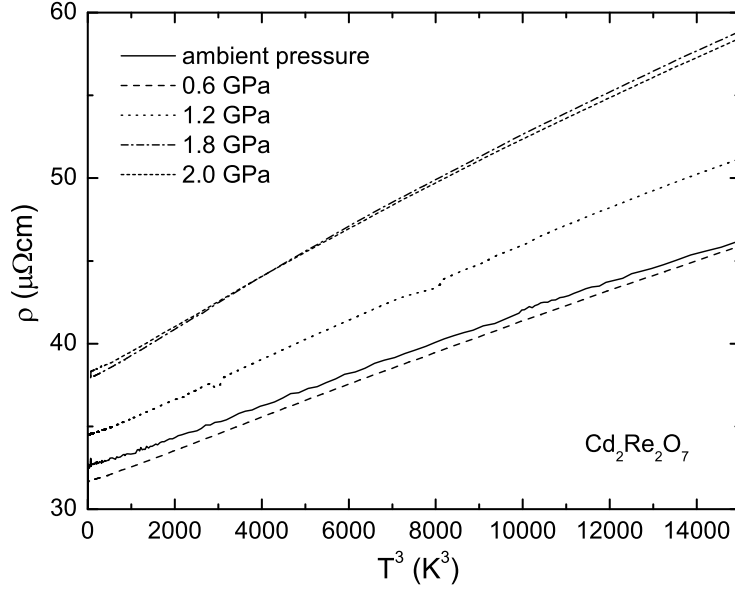


FIG. 11: The resistivity in the range 1–25K, plotted as a function of T^3 .

then appear also as the enhancement of the thermal effective mass $z^{-1} = m^*/m = \gamma^*/\gamma$, and similarly also in the spin susceptibility, and the plasma frequency¹⁸. Much of the previous discussion relied on the idea that the structural transitions open pseudogaps in the spaghetti of t_{2g} subbands, and consequently $\mathcal{N}^*(\epsilon_F)$ is reduced³⁸. This seems to agree with the reduction in susceptibility¹⁹, but makes it difficult to understand why the conductivity is substantially increased. One can argue³⁸ that heavy carriers got eliminated, which at $T > 200\text{K}$ did not contribute to conductivity but rather acted as scatterers. Removing narrow subbands from the vicinity of ϵ_F would mean that $\mathcal{N}(\epsilon_F)$ is reduced. The temperature dependence of χ , the Knight shift and $(TT_1)^{-1}$ measured by ¹¹¹Cd NMR are well described by assuming a reduced $\mathcal{N}(\epsilon_F)$ ²⁷. However, high-resolution photoemission data were interpreted in terms of a low- T enhancement of $\mathcal{N}(\epsilon_F)$ ²⁹.

Our thermopower measurements do not allow to infer $\mathcal{N}(\epsilon_F)$. Using the simplest picture of a correlated one-band model⁴⁰ the thermopower $S \propto -(k_B/|e|)z^{-1}(\mathcal{N}'(\epsilon_F)/\mathcal{N}(\epsilon_F))$ measures the band asymmetry about ϵ_F rather than the density of states. Our data are thus indicative of a strongly increasing asymmetry below 200K. We may envisage a heavy subband gradually crossing out from the vicinity of ϵ_F , which gives a strong contribution to $\mathcal{N}'(\epsilon_F)$.

A pressure–temperature phase diagram based on plotting the characteristic temperatures

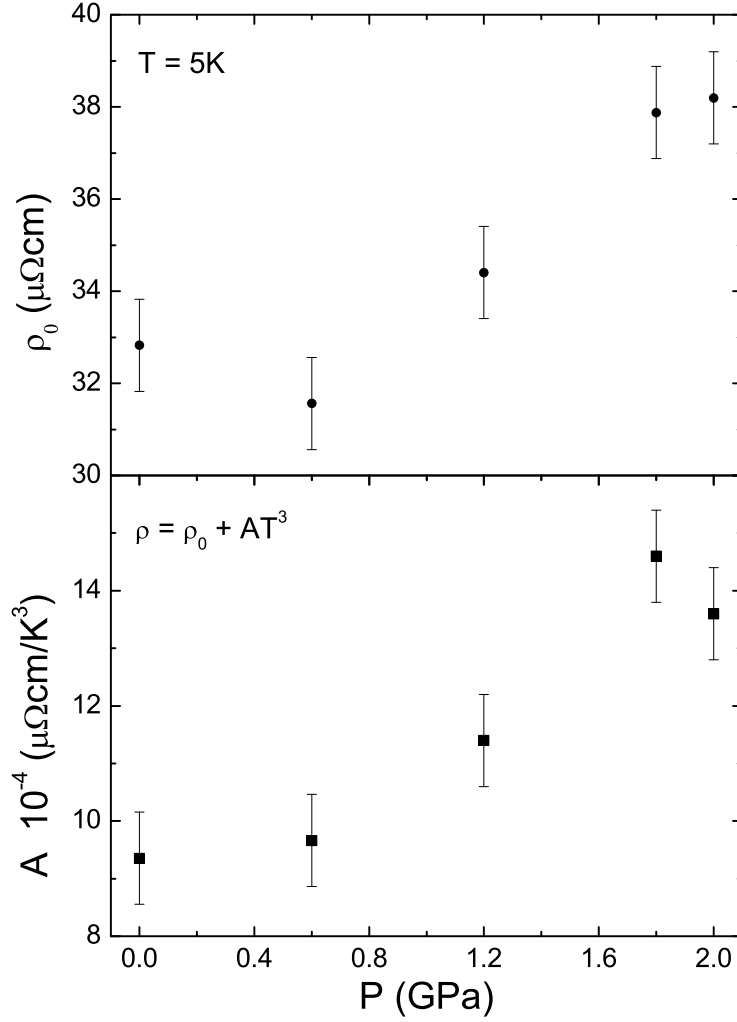


FIG. 12: The pressure dependence of ρ_0 and A_3 .

T_H , T_L , and T^* is shown in Fig. 13. The last data point for T_L at 1.2GPa is, as we have seen, rather tentative; in any case, T_L is suppressed fast. This is in general agreement with a previous observation⁹, but our critical pressure for T_L is rather lower. In contrast, our T_H vs pressure curve would lie above that found by Hiroi et al⁸. T^* is always defined by the peak position of the broad maximum of $d\rho/dT$. It is rather pressure-independent, and approximately coincides with the low- T minimum of S . We do not think it associated with a phase transition but it is nevertheless significant since it marks the crossover from a stable good metallic state into a fluctuating intermediate- T state. We may think of it as the coherence temperature of the low- T electronic structure.

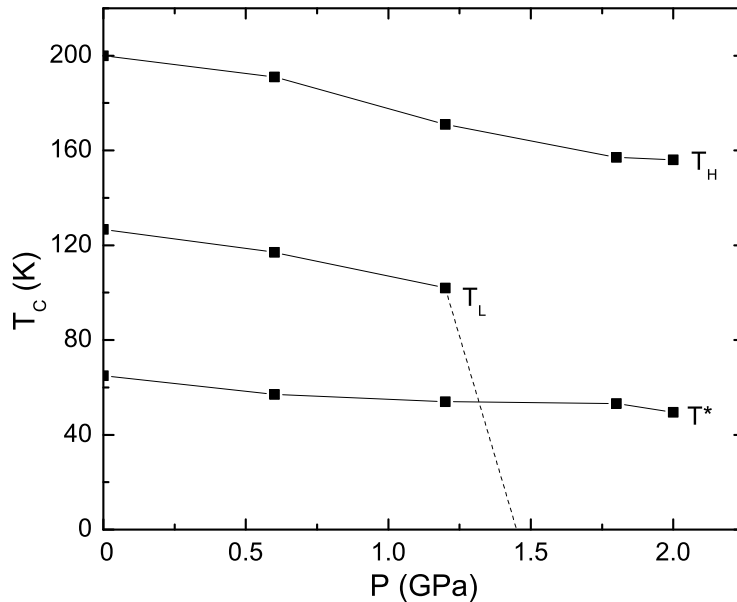


FIG. 13: The T - p phase diagram derived from thermopower and resistivity measurements. Definitions: T_H from the peak in dS/dT ; T_L from the minimum of dS/dT ; T^* is the position of the low- T broad maximum of ρ .

Since we did not find the third normal metallic phase at 1.8 GPa, we drew a dashed line to show that T_L should drop to zero somewhere between 1.2 and 1.8 GPa. In principle, a line of first-order transitions could terminate at a critical point at some finite temperature, but the recent finding of a symmetry change at T_L ²² rules this out: the phase boundary has to continue down to $T = 0$.

One may ask what our final answer is to the question whether $\text{Cd}_2\text{Re}_2\text{O}_7$ is a correlated electron system. Recalling the conflicting inferred results for $\mathcal{N}^*(\epsilon_F)/\mathcal{N}(\epsilon_F)$, we note that seeking the same enhancement factor in various quantities originates from the underlying picture of a one-band model. Having many kinds of spin and orbital correlations (or, alternatively, intra- and inter-subband correlations) should allow a contradiction-free interpretation. The evidence from specific heat alone should suffice to say that $\text{Cd}_2\text{Re}_2\text{O}_7$ is a correlated system. The difficulty that the susceptibility at the same time decreases, may be resolved if we postulate that singlet intersite spin correlations can be induced by electron-electron interaction in a frustrated itinerant system (a similar result was found for the trellis lattice²⁵).

IV. CONCLUSION

We presented resistivity and thermopower measurements on single crystal samples of $\text{Cd}_2\text{Re}_2\text{O}_7$ under five different pressure values up to 2GPa, and used the data to analyze the phase diagram in the T - p plane. The pressure dependence of the thermopower shows that the wide temperature interval between the upper structural transition (at ambient pressure $T_H = 200\text{K}$) and the coherence temperature $T^* \approx 60\text{K}$ is a regime of continuing rearrangement of the electronic structure. The cubic-to-tetragonal transition at 200K does not immediately lead to a stable low-temperature phase, but rather to a state with electronic and structural ambiguity. A particular manifestation of this behavior is the appearance of a second structural phase transition which, is however, confined to relatively low pressures ($< 1.8\text{GPa}$), while the overall features of the system remain the same at higher pressures.

Our results indicate that both coupling to the lattice, and the strongly temperature dependent redistribution of the electrons over the t_{2g} orbital states (or alternatively the t_{2g} subbands) are important for understanding the behavior of this frustrated itinerant system.

Acknowledgments

P.F. is grateful to H. Harima, M. Takigawa, K. Ueda, and O. Vyaselev for enlightening discussions, and acknowledges support by the Hungarian grants OTKA T 038162, OTKA T 037451, and AKP 2000-123 2,2. Work at the University of Tennessee is supported by NSF DMR-0072998. Oak Ridge National Laboratory is managed by UT-Battelle, LLC, for the US Department of Energy under contract DE-AC05-00OR22725. The work in Lausanne was supported by the Swiss National Science Foundation and its NCCR Network "Materials with Novel Electronic Properties".

¹ N.F. Mott: *Metal-Insulator Transitions*, Taylor & Francis Ltd., London (1974).

² P. Fazekas and E. Tosatti: *Phil. Mag. B* **39**, 229 (1979).

³ In the general formula $\text{A}_2\text{B}_2\text{O}_7$, both the A and B sublattices can be envisaged as a network of corner sharing tetrahedra, which is nowadays referred to as the pyrochlore lattice.

⁴ B. Canals and C. Lacroix: *Phys. Rev. Lett.* **80**, 2933 (1998).

- ⁵ R. Moessner and J.T. Chalker: Phys. Rev. Lett. **80**, 2929 (1998).
- ⁶ C. Pinettes, B. Canals and C. Lacroix: Phys. Rev. **B66**, 024422 (2002).
- ⁷ M. Hanawa et al: Phys. Rev. Lett. **87**, 187001 (2001); R. Jin et al.: Phys. Rev. **B64**, 180503 (2001); H. Sakai et al.: J. Phys.: Condens. Mat. **13**, L785 (2001).
- ⁸ Z. Hiroi et al: J. Phys. Soc. Japan **71**, 1553 (2002).
- ⁹ Z. Hiroi and M. Takigawa: Kotaibutsuri (Solid State Physics, in Japanese) **37**, 253 (2002).
- ¹⁰ H. Fukazawa and Y. Maeno: J. Phys. Soc. Japan **71**, 2578 (2002).
- ¹¹ D. Mandrus et al.: Phys. Rev. **B63**, 195104 (2001).
- ¹² W.J. Padilla, D.N. Basov, and D. Mandrus: cond-mat/0201548.
- ¹³ The isotropic Heisenberg model with nearest-neighbour interactions has no ordering transition on the pyrochlore lattice, either for $S=1/2^4$, or for classical spins⁵. The spin liquid phase may be unstable against small perturbations like second neighbour coupling, in which case the question of the kind of spin ordering pattern arises⁶. However, it is difficult to see how a weak effect of this kind could cause a robust metal–insulator transition at 220K.
- ¹⁴ G. Toulouse: Commun. Phys. **2**, 115 (1977).
- ¹⁵ D.J. Singh et al: Phys. Rev. B **65**, 155109 (2002).
- ¹⁶ H. Tsunetsugu: J. Phys. Soc. Japan **71**, 1844 (2002).
- ¹⁷ H. Harima: J. Phys. Chem. Sol. **63**, 1035 (2002).
- ¹⁸ N.L. Wang et al: Phys. Rev. **B66**, 014534 (2002).
- ¹⁹ H. Sakai et al: Phys. Rev. **B66**, 100509(R) (2002).
- ²⁰ H. Tsunetsugu: Phys. Rev. **B65**, 024415 (2001).
- ²¹ Y. Yamashita and K. Ueda: Phys. Rev. Lett. **85**, 4960 (2000).
- ²² J. Yamaura and Z. Hiroi: J. Phys. Soc. Japan **71**, 2598 (2002).
- ²³ Z. Hiroi et al: J. Phys. Soc. Japan **71**, 1634 (2002).
- ²⁴ S. Fujimoto: Phys. Rev. **B64**, 085102 (2001).
- ²⁵ H. Kontani and K. Ueda: Phys. Rev. Lett. **80**, 5619 (1998).
- ²⁶ M. Isoda and S. Mori: J. Phys. Soc. Japan **69**, 1509 (2000).
- ²⁷ O. Vyaselev et al: Phys. Rev. Lett. **89**, 017001 (2002).
- ²⁸ K. Arai et al.: J. Phys.: Condens. Matter **14**, L461 (2002).
- ²⁹ A. Irizawa et al: cond-mat/0207659.
- ³⁰ D. Huo et al.: J. Phys.: Condens. Mat. **14**, L257 (2002).

- ³¹ J.He, R. Jin, and D. Mandrus (unpublished)
- ³² Fig. 1 also shows the superconducting transition at $T_c \approx 1\text{K}$. However, this will not be discussed in this paper, since we could not systematically investigate the superconducting phase under pressure.
- ³³ Strictly speaking, we know only that the overall changes in unit cell dimensions are very small. It may still turn out that individual atomic motions within the unit cell are relatively large, which would allow that the phase transitions are primarily structurally driven (band–Jahn–Teller transitions). However, we take a different view.
- ³⁴ Since the lattice responds to the change in the electronic state, the transitions may be called band–Jahn–Teller transitions. When speaking rather of orbital order, we imply that the phenomenon is primarily driven by electron–electron interactions, and that it would happen even if we held the lattice fixed. A future calculation has to decide if this scenario is correct.
- ³⁵ Using the naive Thomson recipe of equating thermopower with electronic entropy, we would arrive at the fairly small entropy discontinuity 0.08J/K(mole) . This would be in qualitative agreement with the finding by Hiroi *et al*²³.
- ³⁶ The high- T behavior of $\text{Cd}_2\text{Os}_2\text{O}_7$ is pretty much the same, but $\text{Os}^{5+} = 5d^3$ would not have an orbital degree of freedom in the high-spin state. However, allowing for the presence of the low-spin configuration gives orbital degeneracy, and allows the two systems behave similarly.
- ³⁷ J.P. Castellan et al: cond-mat/0201513.
- ³⁸ R. Jin et al: J. Phys.: Condens. Matter **14**, L117 (2002).
- ³⁹ M. Ocko et al.: Phys. Rev. B **64**, 085103 (2001).
- ⁴⁰ J. Merino and R.H. McKenzie: Phys. Rev. B**61**, 7996 (2000).